

# We are IntechOpen, the world's leading publisher of Open Access books Built by scientists, for scientists

**4,800**

Open access books available

**122,000**

International authors and editors

**135M**

Downloads

Our authors are among the

**154**

Countries delivered to

**TOP 1%**

most cited scientists

**12.2%**

Contributors from top 500 universities



**WEB OF SCIENCE™**

Selection of our books indexed in the Book Citation Index  
in Web of Science™ Core Collection (BKCI)

Interested in publishing with us?  
Contact [book.department@intechopen.com](mailto:book.department@intechopen.com)

Numbers displayed above are based on latest data collected.

For more information visit [www.intechopen.com](http://www.intechopen.com)



## 3D RFID Simulation and Design - Factory Automation

Wei Liu and Ming Mao Wong

*\* Singapore Institute of Manufacturing Technology  
Singapore*

*71 Nanyang Drive, Singapore 638075*

### 1. Introduction

The chapter addresses the problem by presenting an analytical model for a 3-dimensional single folded loop antenna with detection coverage in space. Based on the antenna theory, the inductance and impedance of the loop antenna is investigated. Design issues including antenna topology, read range, tag orientations, proximity of metal and other antennas are addressed to determine proper antenna for optimal performance. The proposed design is verified by field distribution measurement and implemented as a RFID reader antenna for a smart shelf application.

#### 1.1 RFID System

Radio Frequency Identification (RFID) is an automatic identification technology that transmits the identity of an object wirelessly using radio waves. It is evolving as a major technology enabler for items tracking and inventory management [1]. The great appeal of RFID technology is that it allows information to be stored and read without requiring either contact or a line of sight between the tag and the reader [2]. Because such technology conveniently dispenses with manual counting of items, it greatly reduces man-made errors and thus improves the accuracy of information.

The RFID system consists of readers (also known as interrogators), tags (also known as transponders), and an information managing host computer [4] shown in Figure 1. In a typical communication sequence, the reader emits a continuous radio frequency (RF) carrier sine wave. When a tag enters the RF field of the reader, the tag receives energy from the field. The tag is composed of an antenna coil and a silicon chip that includes basic modulation circuitry and nonvolatile memory. When the RF field passes through an antenna coil, there is an AC voltage generated across the coil. This voltage is rectified to result in DC voltage for the device operation. The tag becomes functional when the DC voltage reaches a certain level. After the tag has received sufficient energy, it modulates the carrier signal according to the data stored on the tag. Finally, the information is relayed to a host computer.

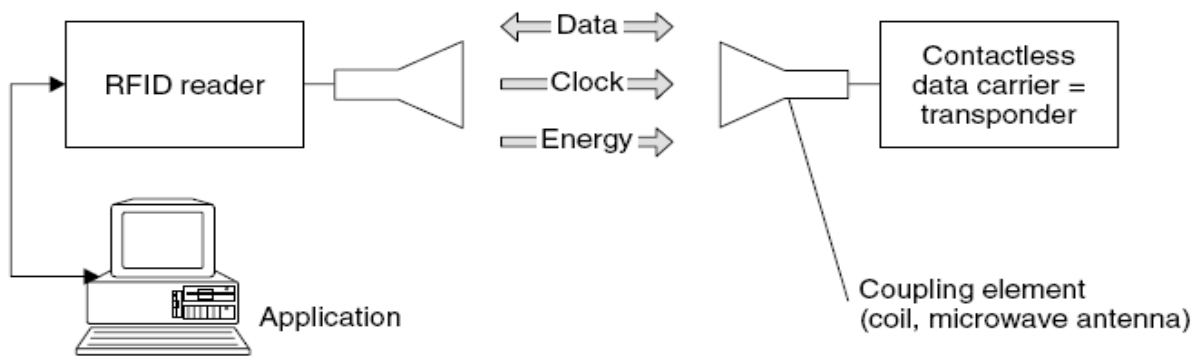


Fig. 1. RFID system

### 1.2 RFID Smart Shelf System

As part of an inventory management in the context of factory, the RFID smart shelf system is extremely useful for tracking of materials. By mounting a RFID reader antenna on each shelf and by placing a passive RFID tag with a unique serial number at each item, it would be possible to detect the presence of the individual item based on the unique serial number associated to it. Users can then query the database to determine the current location of the desired items.

Such a RFID smart shelf system will help to enable a fast, accurate and reliable inventory-checking and eliminates the need for manual stocktaking. Further, the information extracted from the item movements can be used to study usage patterns and detect missing items quickly.

The most common RFID smart shelf application is based on the high frequency (HF) band, which has an As one of RFID applications, the smart shelf system can be useful in maintaining the factory inventory in real time. The system is based on the inductive coupling at 13.56MHz. The read and write range at this frequency is usually not more than 1.5m, and most appropriate for the bookshelf.

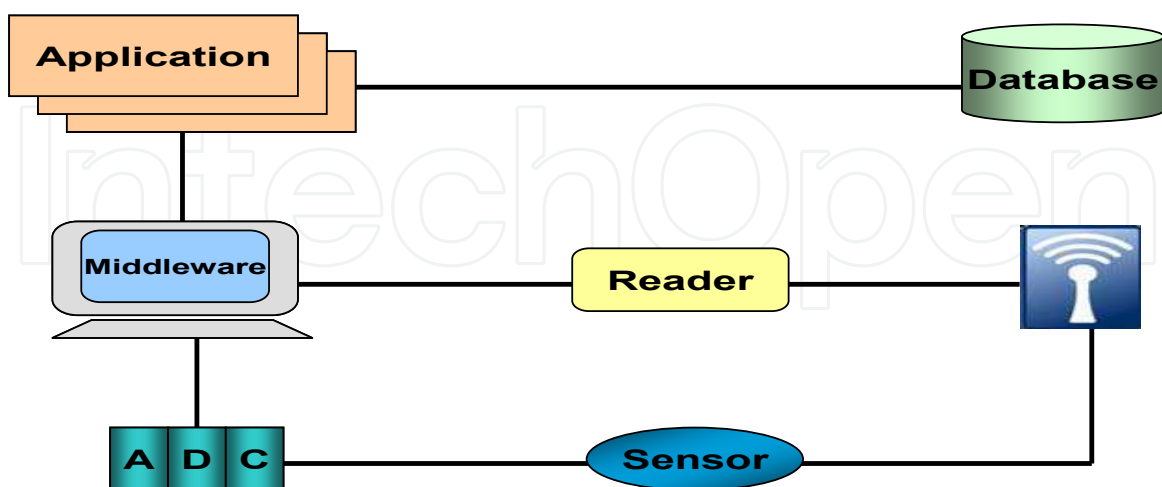


Fig. 2. RFID smart shelf system

Fig. 2. illustrates the components of a RFID smart shelf system. The middleware in the host manages the reader and issues commands. The reader and tag communicate via RF signal.

The tag receives and modifies the carrier signal generated through the reader antenna. The reader receives the modulated signal from the antenna and returns to the middleware. The application reads data from the middleware  $B$ , stores in the database and updates the user interface within the application (Figure 2).

Another feature is associated with the built-in sensor for detecting book movement and thus eliminating the need of constant manual monitoring on the application. The sensor is powered from the energy harvested from the radio wave of a reader. It is integrated with RFID system through Analog Digital Converter (ADC). Figure 7 shows the system implementation.

In order for the RFID system to operate effectively, the antenna plays a very crucial role. The design of the antenna determines the amount of coupling effect, which in turn determines the communication between the reader and the tag. If the antennas of the reader and the tag are not designed correctly, inductive coupling will not occur and the desired tag will not be activated and the whole RFID application to fail.

Among various RFID frequency bands for item level tracking, the most widely used frequency is 13.56 MHz in the high frequency (HF) band. Considering the fact that the wavelength is proportional to the antenna dimensions, designing electrically small antennas in this frequency with a wavelength of 22.12 meters is a very challenging task. To overcome this limitation, a practical and solid RFID reader antenna is proposed with appropriate dimensions as a practical and cheaper alternative [3]. A copper wire single loop antenna was chosen for its ductility, solidity and performance.

Most of the commercially available RFID smart shelf systems can only detect objects (containing RFID tag) effectively in the two-dimensional (2D) field. This requires the reader antennas and tag antennas to be in parallel planes. If they were in other orientations, the reader antenna may not be able to detect the presence of the tag antenna and this will greatly reduce the readability. This restricts the way tagged items can be placed on the shelf and requires multiple antennas to cover a three dimensional region.

The efficiency and performance of the antenna are greatly dependent on its design topology. The structure must be designed such that it can deliver maximum amount of energy to the desired destination in order to achieve efficient antenna performance.

The chapter is divided into four parts.

Part one gives a brief discussion on RFID technology and points out the design limitation for further improvement.

Part two describes the RFID operating principle and antenna design.

Part three details the design methodology of the reader antenna.

Part four concludes the paper and proposes future research.

## 2. Antenna Design

The RFID reader operates in the HF band at 13.56MHz and the reader antenna utilizes the magnetic field to transfer power to the battery-less tag during reading and writing operations. The associated electrical field is not used. The reader expects an antenna to be tuned to a center frequency of 13.56MHz and have an  $50\Omega$  impedance. For optimum performance, the reader matching should have a Voltage Standing Wave Ratio (VSWR) ratio of less than 1.2.

## 2.1 Design Guide

Of all the antennas that can be used to excite a magnetic field, loop antennas are recommended as the most suitable for generating the magnetic field that is required to transfer energy to the HF passive tag. But a number of issues have to be taken into consideration before the design of an antenna can begin.

### 2.1.1 Proximity of Metal

The presence of metal close to an antenna will reduce its performance to some extent. As the antenna is placed close to metal plate, the metal will detune the parameters and also generate eddy current to cancel the EM wave generated by reader [14]. As a result, the read distance will drop. To overcome this, the antenna must be placed a certain amount of distance from the metal.

### 2.1.2 Quality Factor

The performance of an antenna is related with its Quality (Q) factor. In general, the higher the Q, the higher the power output for a particular sized antenna. However, the bandwidth is inversely proportional to the Q [15]. Hence, there should be a maximum value of Q. In the test bed, since the tag operates with a data rate of 70 kHz, the reader antenna circuit needs a bandwidth of at least twice of the data rate. Therefore, it needs:

$$B_{\min} = 140\text{kHz} \quad (1)$$

The Q can be determined by:

$$Q = \frac{f_0}{B} \quad (2)$$

Thus, the maximum attainable Q is obtained from formula (2),

$$Q_{\max} = \frac{13.56\text{MHz}}{140\text{kHz}} = 96.8 \quad (3)$$

### 2.1.3 Presence of Other Antennas

The presence of other antennas will alter the way a system performs because of coupling between the antennas. In this test bed where there are multiple shelves standing together, each embedded with one antenna, there would be interference among these closely placed antennas.

## 2.2 Topology Determination

The parameters of the loop antenna that can be chosen are shape, dimension, number of turns and wire diameter. These will be discussed in the following sections and will lead to a design methodology.

### 2.2.1 Shape

A novel 3-dimensional folded rectangular loop antenna is proposed to generate a magnetic field of at least certain strength within interrogation region. Figure 3 illustrates the schematic of designed antenna topology. The feed-point is located at the base where the electrical current enters and leaves the antenna. The two folded parts of the antenna helps to enhance the magnetic field to detect tags places in different orientations. After entering the feed-point, the current branches into two identical streams which flow through the rest part of the antenna and meet at the exit point. Since the currents flowing through two parallel folded parts are in the same direction, the mutual inductance is positive. Therefore, the magnetic field in x direction is strengthened.

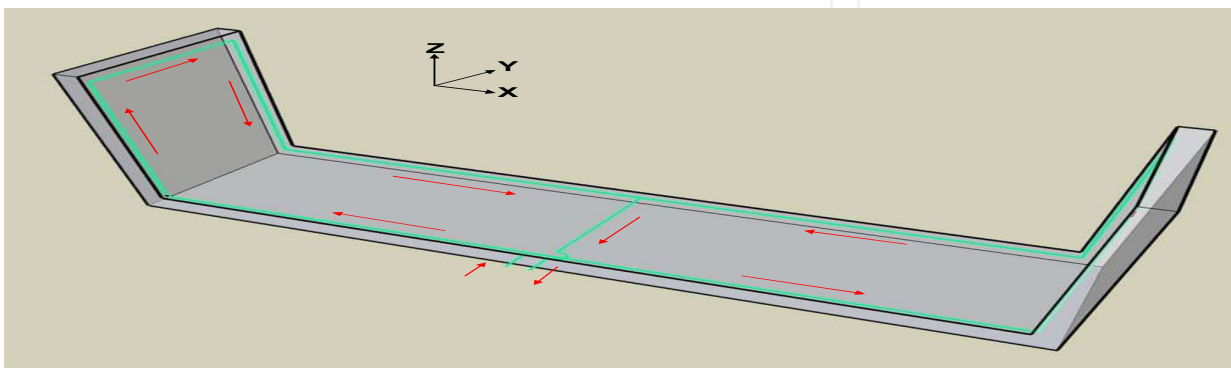


Fig. 2. Antenna topology

### 2.2.2 Number of Turns

For reading a loner ranger, one way is to achieve a larger  $B$  field . This can be done by increasing the number of ampere-turns ( $NI$  ). However, there are drawbacks to this option as the more turns the antenna is, the less portable and more expensive the reader becomes. The consequence of increasing ( $NI$  ) is a larger inductance in the reader antenna circuit that increases as the square of the number of turns. A high inductance load results in large amounts of reflected power (back EMF) as well as a large impedance that varies significantly. Therefore, it is important to keep ( $NI$  ) as small as possible while achieving the minimum  $B$  field needed for the desired read range. For a loop antenna, fed by a voltage source, discarding the small ohm and radiation resistance with respect to  $\omega L$  , the following formula is deduced:

$$\frac{V}{\omega L} = \frac{V}{\omega N L_{N=1}} \propto \frac{V}{N L_{N=1}} \quad (4)$$

where

- $N$  = number of turns
- $I$  = flowing current
- $L_{N=1}$  = inductance of a loop of the same size with only one turn

Hence, to maximize the magnetic field strength  $B$ , we need to maximize  $NL_{N=1}$ , which means  $N = 1$  and keeping  $L_{N=1}$  small.

### 2.2.3 Wire Diameter

Figure 4 illustrates the structure of loop antenna topology.

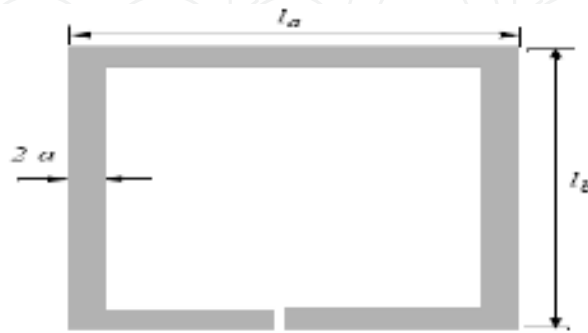


Fig. 4. Inductance of rectangular loop

If reader antenna is made of a rectangular loop composed of a thin wire, its inductance can be calculated by the following formula [16]

$$L_0 = 4 \left\{ l_b \ln \left( \frac{2A}{a(l_b + l_c)} \right) + l_a \ln \left( \frac{2A}{a(l_a + l_c)} \right) + 2[a + l_c - (l_a + l_b)] \right\} \quad (nH) \quad (5)$$

Where the units are all in cm

$a$  = radius of wire

$l_c$  =  $\sqrt{l_a^2 + l_b^2}$

$A$  =  $l_a \times l_b$

Hence, using a wire with a large diameter helps to reduce  $L$ .

### 2.3 Impedance Matching

Since the reader antenna is designed for a smart shelf application, the dimension must fit the mechanical constraints of the bookshelf (100cm\*30cm\*40cm). The magnetic field created by the antenna is used to power the tags associated with the books within the bookshelf and the amount of energy induced in each tag is proportional to the strength of the magnetic field passing through the tag loop. The larger the reader antenna loop is, the more current carrying parts add a contribution to the magnetic field. If the loop becomes too large, however, these contributions become very weak due to the large distance from the current carrying part to the tag. Furthermore, if the total wire length of the loop becomes a considerable part of the wavelength of  $22.12m$ , the standing waves will cause multiple

resonances and decreases the total field [3, 11]. Hence, the antenna dimension is determined experimentally to provide the sufficient magnetic field.

### 2.3.1 Maximum Power Theorem

The antenna and the generator can be represented by an equivalent circuit [17] as shown in Figure 5. The impedance of the antenna is

$$Z_A = R_A + jX_A \quad (6)$$

where

$Z_A$  = antenna impedance at terminals a-b (ohms)

$R_A$  = antenna resistance at terminals a-b (ohms)

$X_A$  = antenna reactance at terminals a-b (ohms)

In general the resistive part of (6) consists of two components; that is

$$R_A = R_r + R_L \quad (7)$$

where

$R_r$  = radiation resistance of the antenna

$R_L$  = loss resistance of the antenna

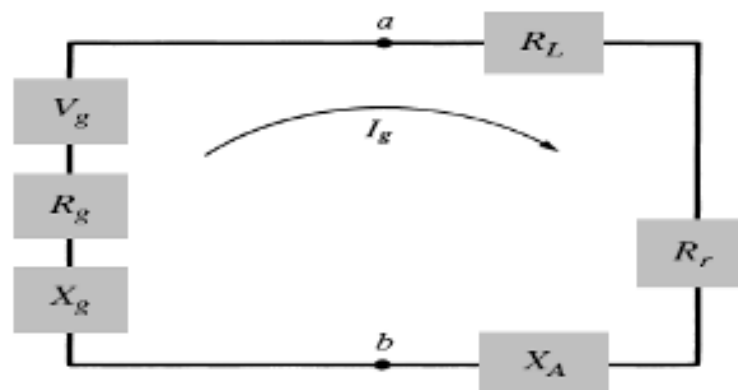


Fig. 5. Antenna equivalent circuit

To find the amount of power delivered to  $R_r$  for radiation and the amount dissipated in  $R_L$  as heat ( $\frac{I^2 R_L}{2}$ ), we first need to find the current developed within the loop which is given by

$$I_g = \frac{V_g}{Z_t} = \frac{V_g}{Z_A + Z_g} = \frac{V_g}{(R_r + R_L + R_g) + j(X_A + X_g)} \quad (A) \quad (8)$$



and its magnitude by

$$|I_g| = \frac{|V_g|}{\left[ (R_r + R_L + R_g)^2 + (X_A + X_g)^2 \right]^{\frac{1}{2}}} \quad (9)$$

where  $V_g$  is the peak generator voltage. The power delivered to the antenna for radiation is given by

$$P_r = \frac{1}{2} |I_g|^2 R_r = \frac{|V_g|^2}{2} \left[ \frac{R_r}{(R_r + R_L + R_g)^2 + (X_A + X_g)^2} \right] \quad (A) \quad (10)$$

and the dissipated as heat by

$$P_L = \frac{1}{2} |I_g|^2 R_L = \frac{|V_g|^2}{2} \left[ \frac{R_L}{(R_r + R_L + R_g)^2 + (X_A + X_g)^2} \right] \quad (W) \quad (11)$$

The remaining power is dissipated as heat on the internal resistance  $R_g$  of the generator, and it is given by

$$P_g = \frac{|V_g|^2}{2} \left[ \frac{R_g}{(R_r + R_L + R_g)^2 + (X_A + X_g)^2} \right] \quad (W) \quad (12)$$

The maximum power delivered to the antenna occurs when we have conjugate matching; that is when

$$R_r + R_L = R_g \quad (13)$$

$$X_A = -X_g \quad (14)$$

For this case

$$P_g = P_r + P_L = \frac{|V_g|^2}{8} \left[ \frac{R_g}{(R_r + R_L)^2} \right] = \frac{|V_g|^2}{8} \left[ \frac{R_r + R_L}{(R_r + R_L)^2} \right] \quad (15)$$

The power supplied by the generator during conjugate matching is

$$P_s = \frac{1}{2} V_g I_g^* = \frac{1}{2} V_g \left[ \frac{V_g^*}{2(R_r + R_L)} \right] = \frac{|V_g|^2}{4} \left[ \frac{1}{(R_r + R_L)} \right] \quad (16)$$

Of the power that is provided by the generator, half is dissipated as heat in the internal resistance ( $R_g$ ) of the generator and the other half is delivered to the antenna. This only happens when conjugate matching is applied.

### 2.3.2 Two-Component Matching Network

Figure 6 displays the antenna impedance, which is  $1.585 + j119.74(\Omega)$  at 13.56MHz. In order to achieve maximum power transfer, it is required to match the impedance of the load to that of the source ( $50\Omega$ ). This is accomplished by incorporating additional passive networks connected in between source and load.

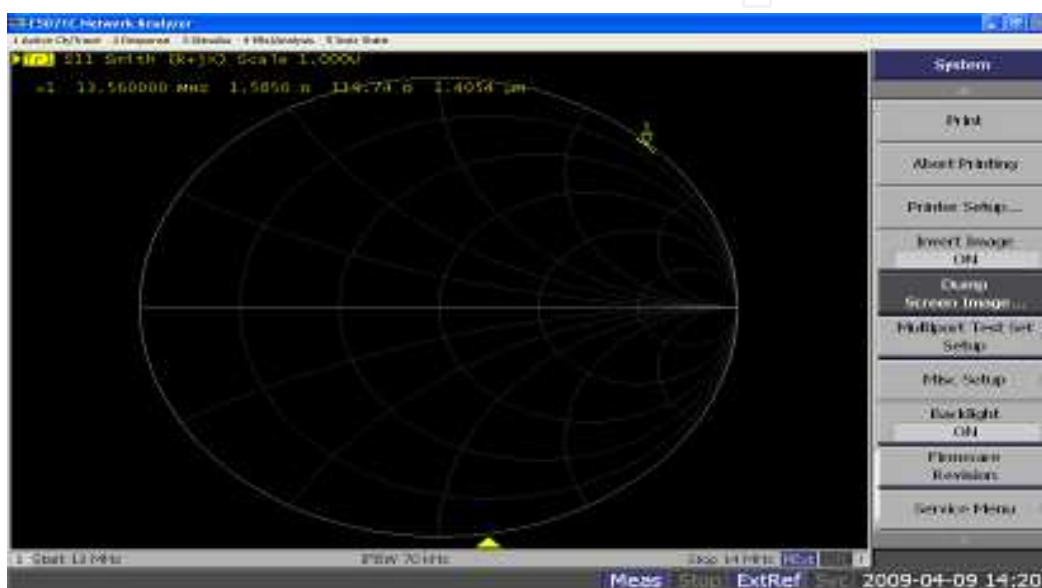


Fig. 6. Antenna impedance without matching network

The two-component network [18], also known as L-type due to the element arrangement, is used to transform the load impedance ( $Z_{load}$ ) to the desired input impedance ( $Z_{in}$ ). The components are alternatively connected in series and shunt configuration, as shown in Figure 7, which depicts eight possible arrangements of capacitors and inductors.

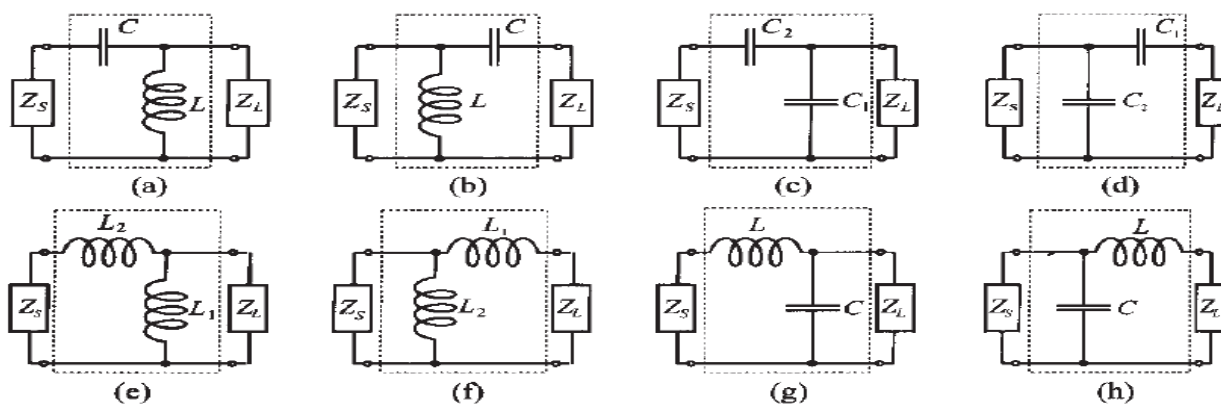


Fig. 7. Eight possible configurations of the two-component matching networks

There are two broad approaches in designing a matching network.

- To derive the values of the elements analytically
- To rely on the Smith Chart as a graphical design tool

The first approach yields very precise results. Alternatively, the second approach is more intuitive, easier to verify, and faster for an initial design, since it does not require complicated computations. Both approaches are applied as a cross-checking.

### 2.3.3 Analytical Approach

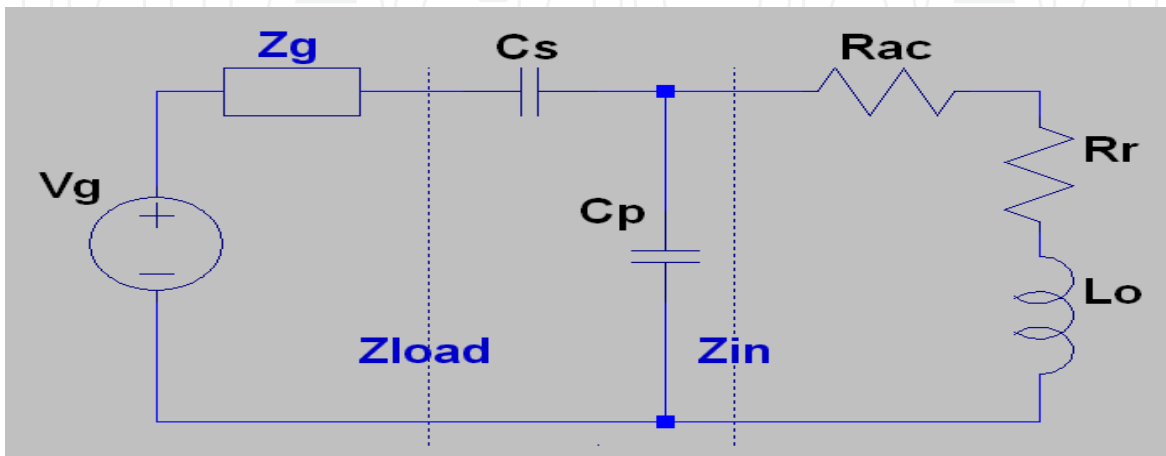


Fig. 8. L-type matching network design

As shown in Figure 8, the small loop antenna is primarily inductive and it can be represented by a lumped element equivalent circuit [17].

$$Z_{in} = R_{in} + jX_{in} = (R_r + R_{ac}) + jX_L \quad (17)$$

where

$R_r$  = radiation resistance

$R_{ac}$  = AC resistance of loop conductor

$X_L$  = inductive reactance =  $\omega L_0$

The capacitors  $C_s, C_p$  are used to tune the antenna impedance to be  $50\Omega$  for maximum power efficiency. This is accomplished by choosing  $C_s, C_p$  according to

$$(-jX_s) + \frac{1}{\frac{j}{X_p} + \frac{1}{R_{in} + jX_{in}}} = 50 \quad (\Omega) \quad (18)$$

$$(-jX_s) + \frac{1}{\frac{jR_{in} - X_{in} + X_p}{X_p(R_{in} + jX_{in})}} = 50 \quad (\Omega) \quad (19)$$

$$(-jX_s) + \frac{X_p(R_{in} + jX_{in})(X_p - X_{in} - jR_{in})}{(X_p - X_{in})^2 + R_{in}^2} = 50 \quad (\Omega) \quad (20)$$

$$(-jX_s) + \frac{X_p^2 R_{in} + j(X_{in} X_p^2 - X_{in}^2 X_p - X_p R_{in}^2)}{(X_p - X_{in})^2 + R_{in}^2} = 50 \quad (\Omega) \quad (21)$$

The real part is

$$\frac{X_p^2 R_{in}}{(X_p - X_{in})^2 + R_{in}^2} = 50 \quad (22)$$

The imaginary part cancels out

$$\frac{X_{in} X_p^2 - X_{in}^2 X_p - X_p R_{in}^2}{(X_p - X_{in})^2 + R_{in}^2} = X_s \quad (23)$$

Given  $R_{in} = 1.585$ ,  $X_{in} = 119.74$ , it is calculated that  $X_s = 670.7$ ,  $X_p = 145.8$ , which is  $C_s = 17.5 \text{ pF}$ ,  $C_p = 80.5 \text{ pF}$ .

### 2.3.4 Graphical Approach

The Smith Chart is used for rapid and relatively precise designs of the matching circuits. The appeal of this approach is that its complexity remains almost the same independent of the number of components in the network. Moreover, the parameter choice and its value assignment can be instantaneously displayed at part of the Smith Chart on the computer screen.

Figure 9 illustrates the steps of L-type matching network design by using the Smith Chart as a graphical tool. The initial data point  $Z_L$  is  $1.585 + j119.74$ . Since the first component is a shunt capacitor  $C_p$ , the total impedance of this parallel combination is positioned somewhere on the circle of constant conductance in green color that passes through the point  $Z_L$ . Next, the second capacitor  $C_s$  is added in series with the parallel combination of  $Z_L$  and  $C_p$ . The resulting impedance will move along the circle of constant resistance in red color. For maximum power gain it is required that an output impedance of the matching network connected to the antenna to be equal to the complex conjugate of the transmitter impedance. This circle has to pass through the center of the Smith Chart which is  $50 \Omega$ .

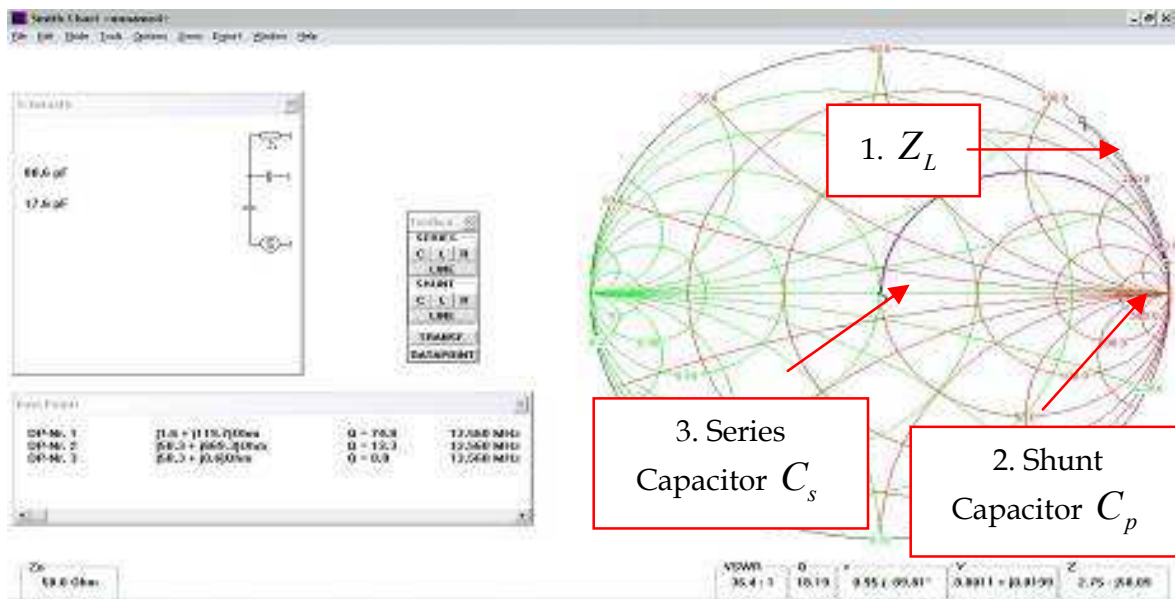


Fig. 9. Matching network design with Smith Chart

The intersection of two circles in the Smith Chart determines the impedance formed by the shunt connection of antenna and capacitor. Reading from the Smith Chart, it is found that this impedance is approximately

$$Z_{LC} = 49.4 + j666.86$$

The corresponding admittance is

$$Y_{LC} = 1.1 \times 10^{-4} + j1.5 \times 10^{-3}$$

The admittance of antenna is

$$Y_L = 1.1 \times 10^{-4} + j8.35 \times 10^{-3}$$

Therefore, the susceptance of the shunt capacitor is  $jB_p = Y_{LC} - Y_L = j6.85 \times 10^{-3}$ . The reactance of the series capacitor is  $-jX_s = 50 - Z_{LC} = -j666.86$ . Finally, the actual values are  $C_s = 17.5 \text{ pF}$ ,  $C_p = 80.5 \text{ pF}$ .

The results of both analytical and graphical approaches were found to correlate quite well.

### 3. Antenna Methodology Development

The 3-dimensional single-loop antenna is built using coated copper wire as shown in Figure 10. The diameter of electrical wire is expressed as the American Wire Gauge (AWG) number. The gauge number is inversely proportional to diameter, and the diameter is

roughly doubled every six wire gauges. Since there is no coated wire for AWG 1-7, AWG 8 is the best choice available with largest diameter.

The antenna is then attached to a piece of foam base to give the antenna rigidity and mechanical support. Without the foam base, the structure of the antenna may not be uniform throughout the testing process (bending of wire etc) and this will have an undesirable impact on the inductance of the antenna and in turn may cause the antenna to be unreliable. Foam is chosen as it is a non-metallic material therefore it will not have any magnetic effect on the antenna. The feed point is made in the middle of the antenna and it will be used to provide interface with the RFID reader/writer.



Fig. 3. Prototype of RFID reader antenna

The theoretical derivation provides a good guide to implement the matching network. In practice, a variable capacitor with a large range e.g.  $12-80\text{ pF}$  is used to achieve the desired range. Once the matching has been achieved, it is removed and measured and a larger fixed capacitor is used, together with a smaller variable capacitor, to allow for fine turning. Figure 11 shows the actual L-type matching network where the series branch consists of one fixed capacitor of  $5\text{ pF}$  with one variable capacitor of  $3-11\text{ pF}$  and the shunt branch is composed of two parallel capacitors of  $47\text{ pF}$  each with one variable capacitor of  $3-11\text{ pF}$  as well.

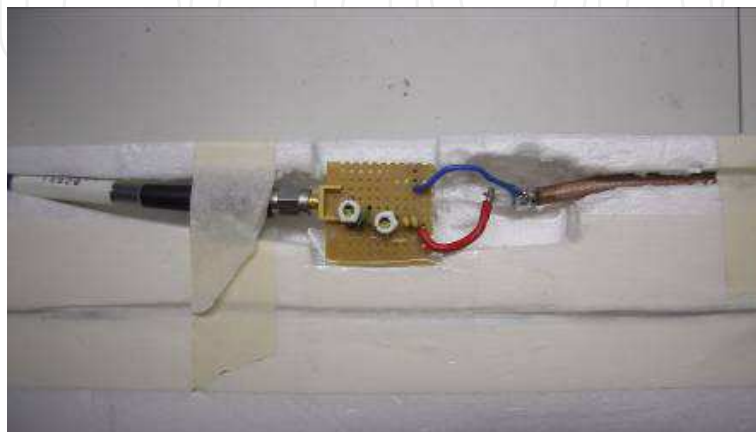


Fig. 4. L-type matching network



### 3.1 Antenna Measurement

The antenna performance is assessed by measuring following parameters.

#### 3.1.1 Return Loss and SWR

After the antenna is connected to the matching circuit and fine tuned and matched to 50 ohms, we measured the impedance and SWR value of the antenna. Figure 12 displays the impedance is around  $50\ \Omega$ . And the antenna has a return loss is  $-14.785\text{dB}$  and SWR is 1.0828 as show in Figure 13.

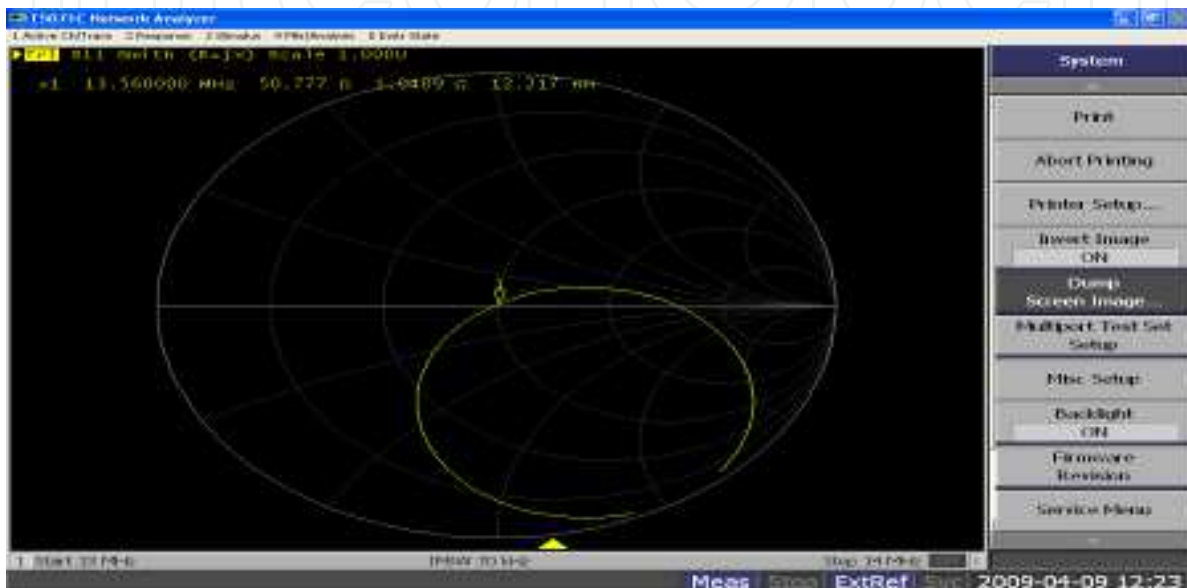


Fig. 12. Antenna impedance with matching network

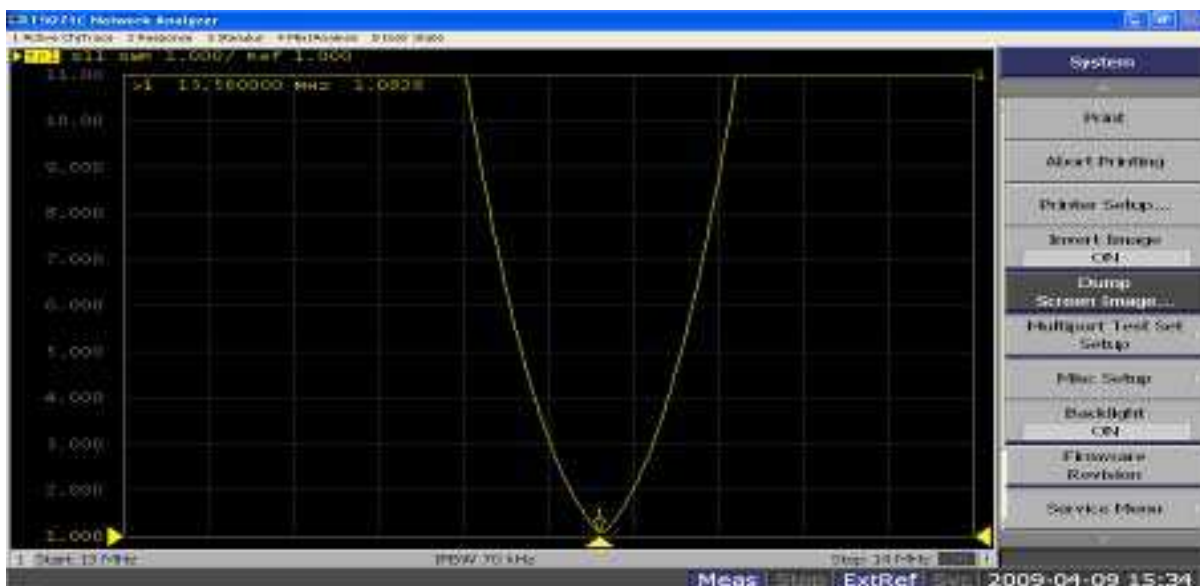


Fig. 13. Antenna SWR

Both results indicate that maximum amount of energy are transmitted to the antenna and this will ensure that data loss are reduced to the minimum.

### 3.1.2 Quality Factor

The Q factor represents the amount of AC resistance of a system at resonance and it can be determined by measuring the 3-dB bandwidth of the antennas' near field response, frequency sweep between 13 MHz and 14 MHz.

Figure 14 displays the measurement of Q factor. At 13.56MHz labeled by marker 2, the antenna exhibits the resonance. At 13.46MHz and 13.66MHz, the lower and upper -3dB points are found and recorded.

The three frequencies can be used in the formula (2):

$$Q = \frac{f_0}{f_2 - f_1} = \frac{13.56}{13.66 - 13.46} = 67.8 \quad (24)$$

The Q value is smaller than the upper limit 96.8.

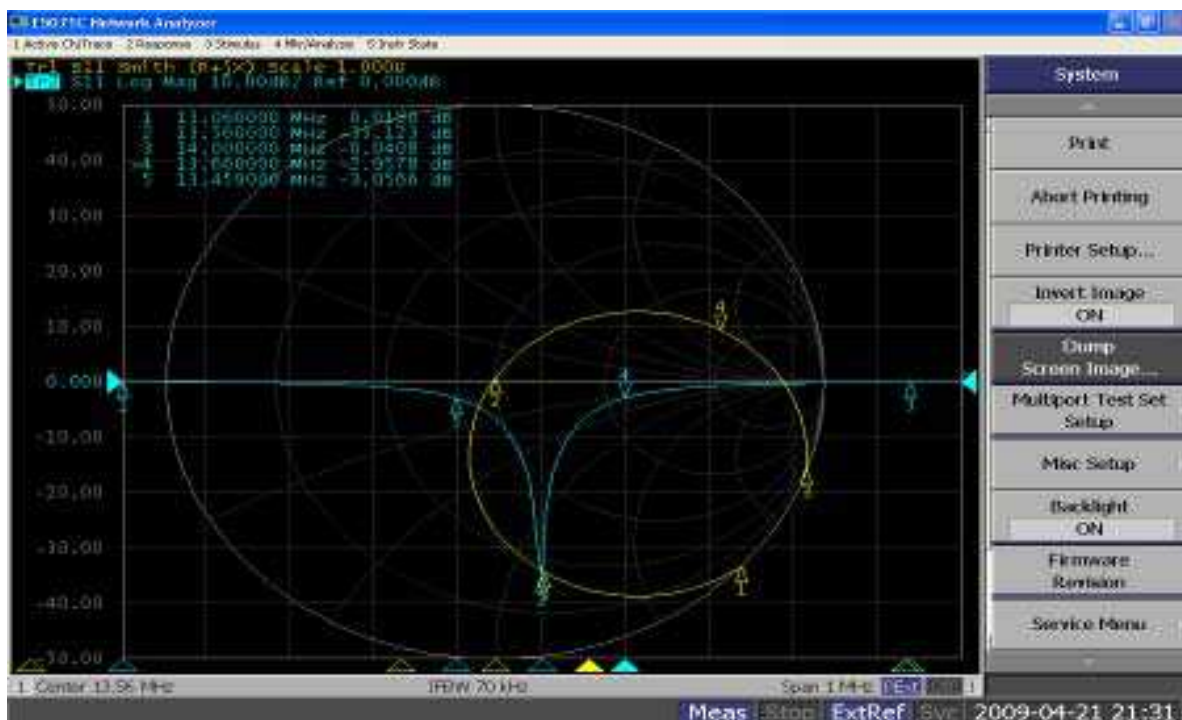


Fig. 14. Q factor measurement

### 3.1.3 Field Distribution Measurement

The antenna model must be able to produce an electromagnetic field having a magnitude of at least an interrogation threshold of a tag for the entire interrogation region.

The magnetic field strength of the loop antenna at a specified distance determines the reading range of an RFID system with prior selected RFID reader and tag. The stronger the magnetic field, the larger the detection range. Strength of the measured field is represented by the induced voltage. The tag utilized in the experiment is activated only when the induced voltage is greater than 200mV. Magnetic field intensity of the loop antennas is measured at varying test points [19]. The measurement is conducted by using oscilloscope as shown in Figure 15.



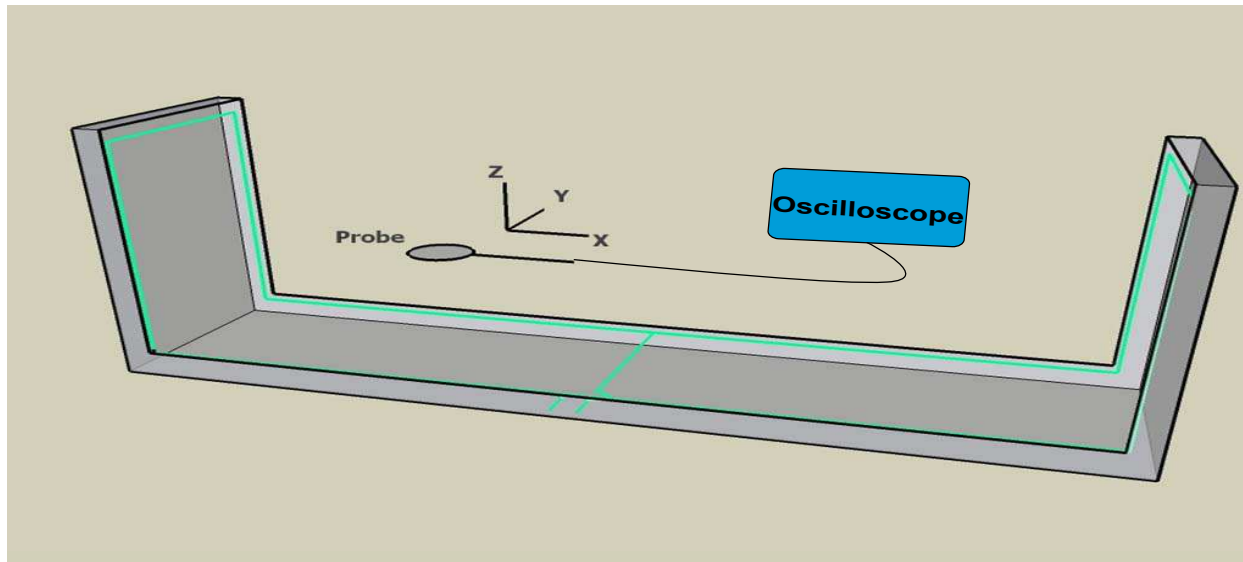


Fig. 15. Setup for field distribution measurement

Figure 16 shows that at the mid cross section  $x = 44$  cm of the antenna, the field distribution in X-direction varies significantly with the z coordinate. The loop antenna generates strong magnetic field in the region closer to the antenna ( $z \leq 20$  cm), while the field decreases as distance from the antenna increases. The antenna is able to detect the tag within 30 cm height of the antenna.

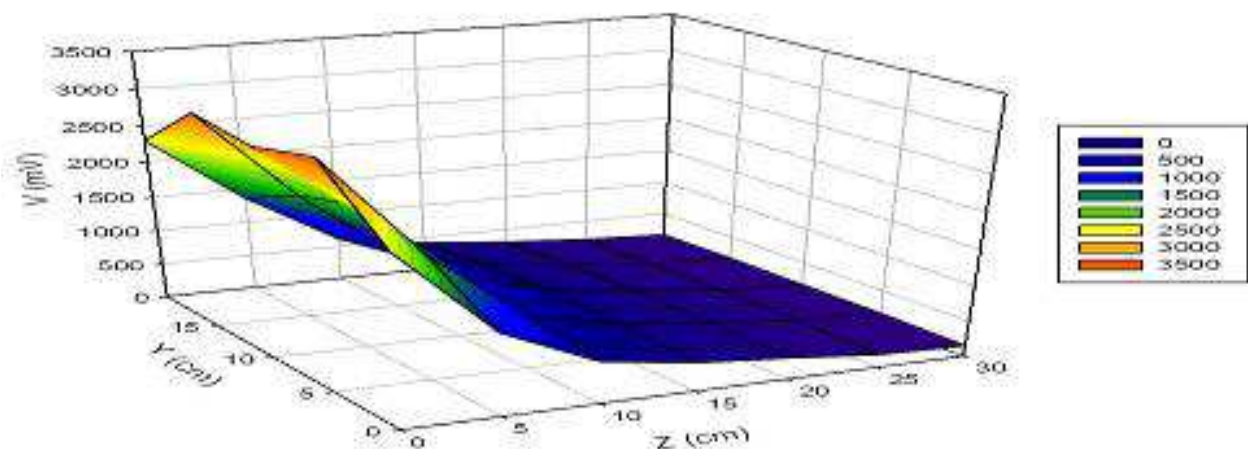


Fig. 16. Magnetic field distribution in x direction

Figure 17 presents that across the mid plane  $y = 20$  cm of the antenna, the magnetic field in Y-direction slightly achieves the peak values at both edges of and slightly drops in the middle of the antenna for the same height. As distance from the antenna increases, the field decreases. There is a black region between  $x = 33$  cm and  $x = 55$  cm as  $z \geq 15$  cm.

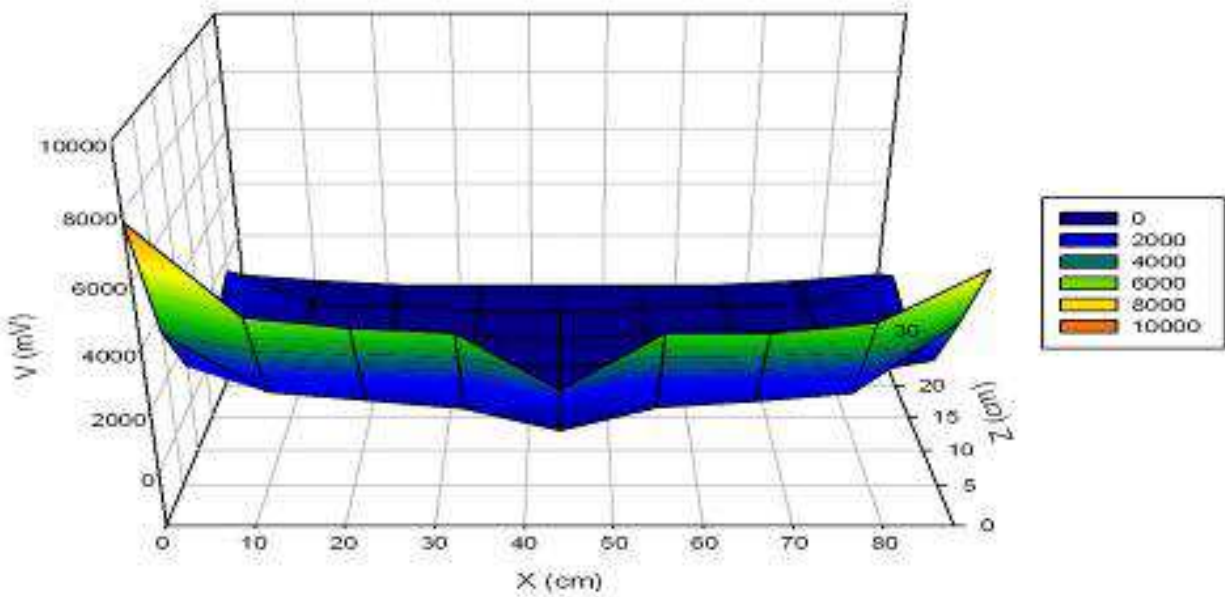


Fig. 17. Magnetic Field distribution in y direction

Figure 18 illustrates the magnetic field distribution in Z-direction across the plane  $z = 18$  cm above the antenna. The antenna produces strong magnetic field at both edges. There is a black region in the middle of the antenna.

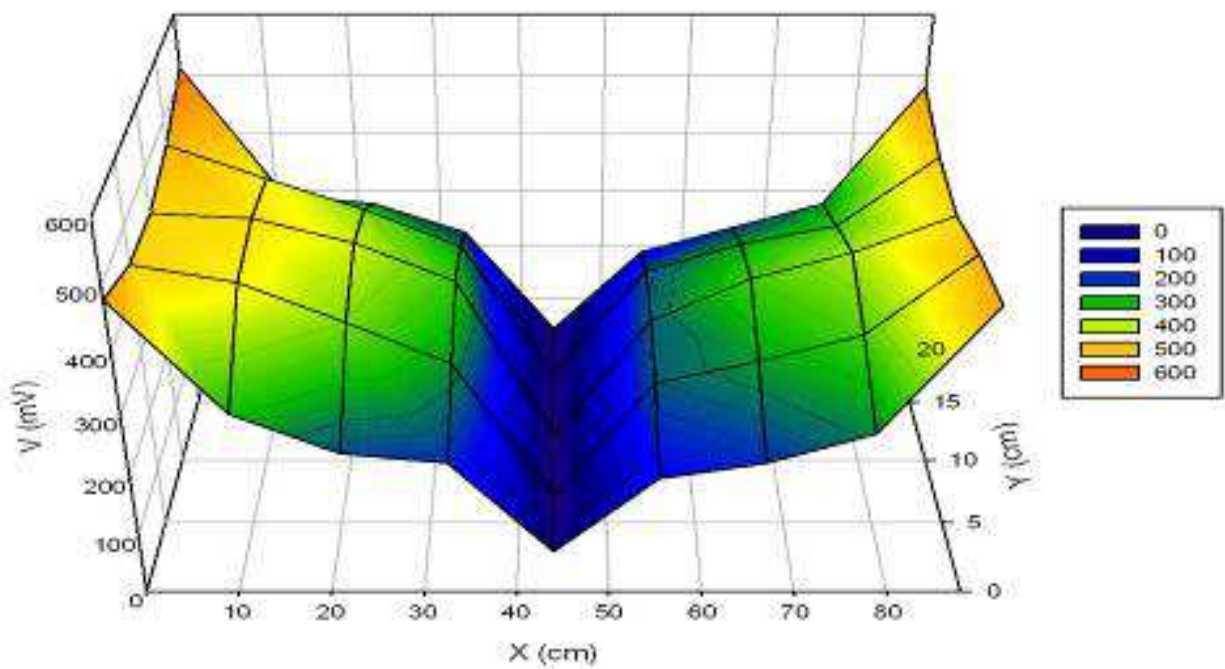


Fig. 18. Three-dimensional field distribution in z direction

### 3.1.4 Antenna Read Distance

Figure 19 illustrates the magnetic field intensity in x direction measured by moving the tag along three different lines, starting from points  $(y = 10, z = 5)$ ,  $(y = 10, z = 15)$ ,  $(y = 10, z = 25)$ . These three lines are representative of all positions where the books are placed vertically. The magnetic field intensity is strong at both sides but drops rapidly as moving towards the center. In the middle of the antenna, the field becomes strong again.

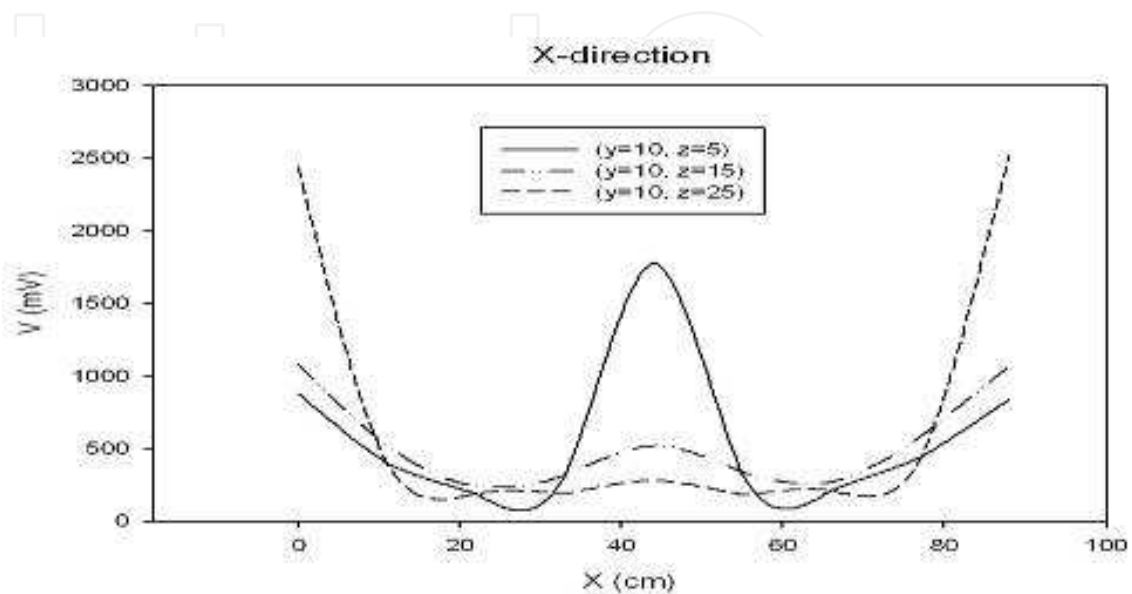


Fig. 19. Magnetic field intensity along different lines in x direction

Figure 20 shows the magnetic field intensity in y direction measured by moving the tag along three different lines, starting from points  $(x = 22, z = 15)$ ,  $(x = 44, z = 15)$ ,  $(x = 66, z = 15)$ . These three lines are representative of typical positions where books are placed perpendicularly. The two lines in the upper region of the diagram differ in the trace of the line in the lower region.

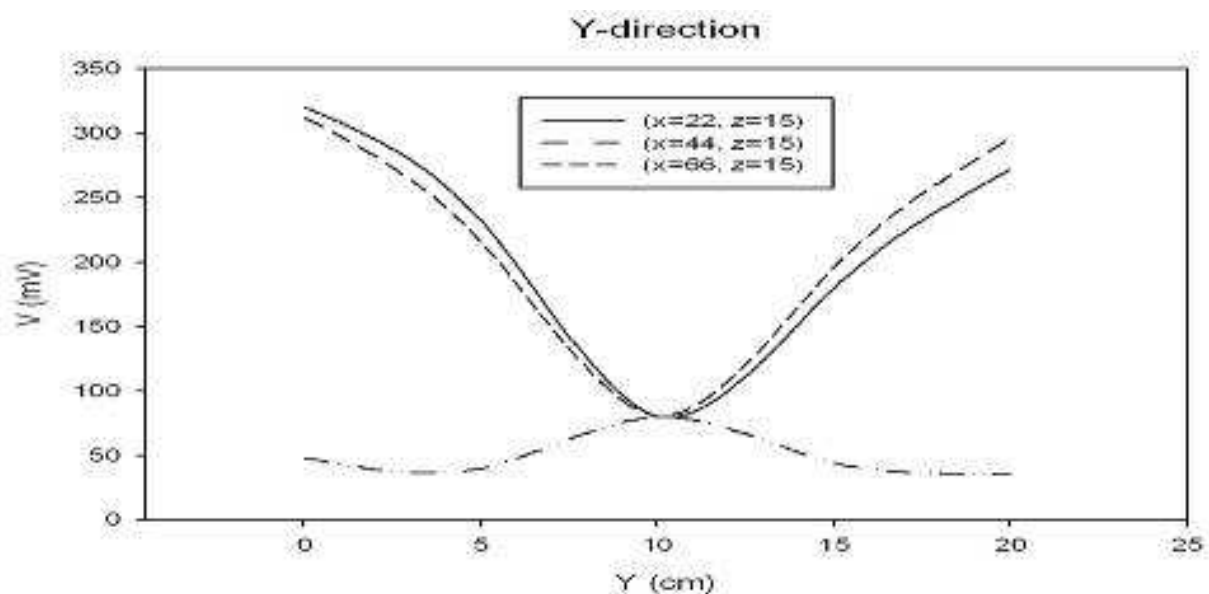


Fig. 20. Magnetic field intensity along different lines in y direction

Figure 21 presents the magnetic field intensity in z direction measured by moving the tag along three different lines, starting from points  $(x = 22, y = 10)$ ,  $(x = 44, z = 10)$ ,  $(x = 66, z = 10)$ . These three lines are representative of typical positions where books are placed horizontally. The further away from the antenna, the weaker the field becomes.

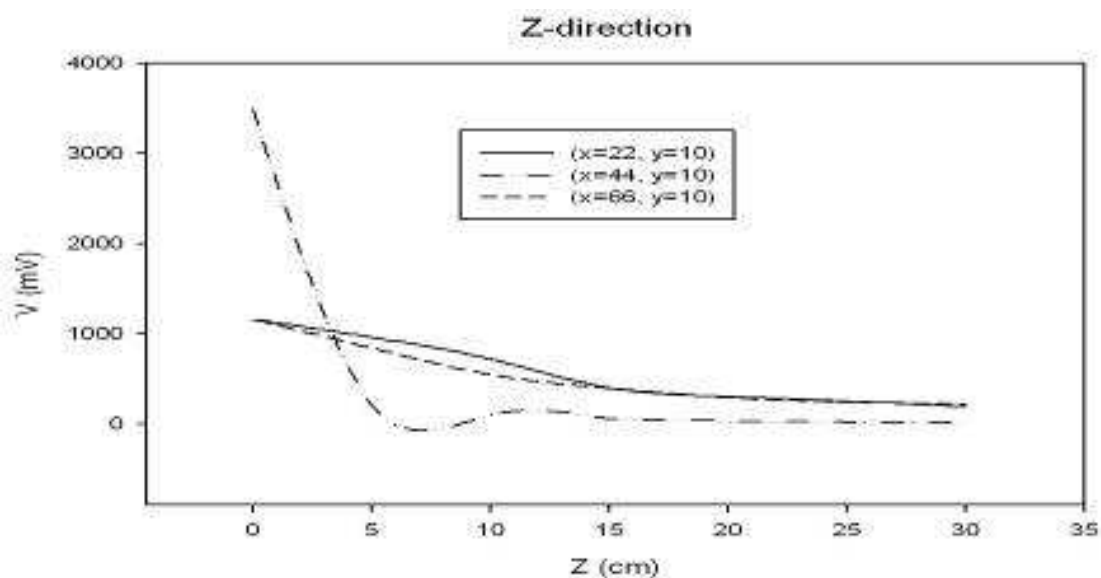


Fig. 21. Magnetic field intensity along different lines in z direction

### 3.1.5 Various Orientations

The results from the above sections were then used to develop a prototype for RFID book shelf application. The prototype was able to detect books in a number of different orientations within the 3D region with a range of 44 cm from the vertical antenna as shown in Figure 22.



Fig. 22. prototype of smart book shelf

## 4. Conclusion

This chapter has presented and investigated loop antenna and sensor circuit for HF RFID smart shelf application.

The issues including tag orientations, read range, proximity of metal and other antennas are approached during the antenna design. A 3-dimensional shape of single turn loop antenna is proposed. The optimum antenna size was determined as a trade-off between the magnetic field strength and mechanical constraint. The antenna model has been successfully used to configure an HF RFID smart shelf prototype. The performance test has shown that the antenna is capable of achieving the desired results.

The further research following this project would involve integrating more than one bookshelf into the smart shelf application.

## 5. Reference

- [1] J. Landt, "The history of RFID," *Potentials, IEEE*, vol. 24, pp. 8-11, 2005.
- [2] R. Want, *RFID Explained: A Primer on Radio Frequency Identification Technologies*: Morgan & Claypool Publishers, 2006.
- [3] D. Miron, *Small Antenna Design*: Newnes, 2006.
- [4] K. Finkenzeller, *RFID Handbook: Fundamentals and Applications in Contactless Smart Cards and Identification*, 2nd ed. New York: Wiley, 2003.
- [5] V. Chawla and H. Dong Sam, "An overview of passive RFID," *Communications Magazine, IEEE*, vol. 45, pp. 11-17, 2007.
- [6] F. Fuschini, C. Piersanti, F. Paolazzi, and G. Falciasecca, "On the Efficiency of Load Modulation in RFID Systems Operating in Real Environment," *Antennas and Wireless Propagation Letters, IEEE*, vol. 7, pp. 243-246, 2008.
- [7] H. K. Ryu and J. M. Woo, "Miniaturisation of rectangular loop antenna using meander line for RFID tags," *Electronics Letters*, vol. 43, pp. 372-374, 2007.
- [8] S. C. Q. Chen and V. Thomas, "Optimization of inductive RFID technology," in *Electronics and the Environment, 2001. Proceedings of the 2001 IEEE International Symposium on*, 2001, pp. 82-87.
- [9] J. Nummela, L. Ukkonen, L. Sydanheimo, and M. Kivikoski, "13,56 MHz RFID antenna for cell phone integrated reader," in *Antennas and Propagation Society International Symposium, 2007 IEEE*, 2007, pp. 1088-1091.
- [10] T. Instruments, "HF Antenna Design Notes Technical Application Report," 11-08-26-003, September 2003.
- [11] W. Aerts, E. De Mulder, B. Preneel, G. A. E. Vandenbosch, and I. Verbauwhede, "Dependence of RFID Reader Antenna Design on Read Out Distance," *Antennas and Propagation, IEEE Transactions on*, vol. 56, pp. 3829-3837, 2008.
- [12] C. Klaf, A. Missoni, G. Hofer, G. Holweg, and W. Kargl, "Improvements in Operational Distance in passive HF RFID Transponder Systems," in *RFID, 2008 IEEE International Conference on*, 2008, pp. 250-257.
- [13] D. C. Yates, A. S. Holmes, and A. J. Burdett, "Optimal transmission frequency for ultralow-power short-range radio links," *Circuits and Systems I: Regular Papers, IEEE Transactions on*, vol. 51, pp. 1405-1413, 2004.

- [14] Q. Xianming and C. Zhi Ning, "Proximity Effects of Metallic Environments on High Frequency RFID Reader Antenna: Study and Applications," *Antennas and Propagation, IEEE Transactions on*, vol. 55, pp. 3105-3111, 2007.
- [15] S. R. Best, "A discussion on the quality factor of impedance matched electrically small wire antennas," *Antennas and Propagation, IEEE Transactions on*, vol. 53, pp. 502-508, 2005.
- [16] Y. Lee and P. Sorrells, "AN680: MicroID 13.56 MHz RFID System Design Guide," Microchip Technology Inc., 2004.
- [17] C. A. Balanis, *Antenna Theory: Analysis and Design*, 3rd ed. Hoboken, N.J.: Wiley-Interscience, 2005.
- [18] R. Ludwig, P. Bretchko, and G. Bogdanov, *RF Circuit Design: Theory and Applications*, 2nd ed.: Prentice Hall, 2007.
- [19] A. Cai, Q. Xianming, C. Zhi Ning, and L. Boon Keng, "Performance assessment of printed RFID reader antenna," in *Antennas and Propagation Society International Symposium, 2007 IEEE*, 2007, pp. 301-304.
- [20] Noax, "Experiment #52 – SWR Meters," *QST*, May 2007.
- [21] C. Bowick, *RF Circuit Design*. Burlington, MA: Newnes, 1997.

IntechOpen



IntechOpen

IntechOpen



## **Factory Automation**

Edited by Javier Silvestre-Blanes

ISBN 978-953-307-024-7

Hard cover, 602 pages

**Publisher** InTech

**Published online** 01, March, 2010

**Published in print edition** March, 2010

Factory automation has evolved significantly in the last few decades, and is today a complex, interdisciplinary, scientific area. In this book a selection of papers on topics related to factory automation is presented, covering a broad spectrum, so that the reader may become familiar with the various fields, and also study them in more depth where required. Within various chapters in this book, special attention is given to distributed applications and their use of networks, since it is one of the most relevant subjects in the evolution of factory automation. Different Medium Access Control and networks are analyzed, while Ethernet and Wireless networks are looked at in more detail, since they are among the hottest topics in recent research. Another important subject is everything concerning the increase in the complexity of factory automation, and the need for flexibility and interoperability. Finally the use of multi-agent systems, advanced control, formal methods, or the application in this field of RFID, are additional examples of the ideas and disciplines that experts around the world have analyzed in their work.

### **How to reference**

In order to correctly reference this scholarly work, feel free to copy and paste the following:

Wei Liu and Ming Mao Wong (2010). 3D RFID Simulation and Design - Factory Automation, Factory Automation, Javier Silvestre-Blanes (Ed.), ISBN: 978-953-307-024-7, InTech, Available from:  
<http://www.intechopen.com/books/factory-automation/3d-rfid-simulation-and-design-factory-automation>

**INTECH**  
open science | open minds

### **InTech Europe**

University Campus STeP Ri  
Slavka Krautzeka 83/A  
51000 Rijeka, Croatia  
Phone: +385 (51) 770 447  
Fax: +385 (51) 686 166  
[www.intechopen.com](http://www.intechopen.com)

### **InTech China**

Unit 405, Office Block, Hotel Equatorial Shanghai  
No.65, Yan An Road (West), Shanghai, 200040, China  
中国上海市延安西路65号上海国际贵都大饭店办公楼405单元  
Phone: +86-21-62489820  
Fax: +86-21-62489821



© 2010 The Author(s). Licensee IntechOpen. This chapter is distributed under the terms of the [Creative Commons Attribution-NonCommercial-ShareAlike-3.0 License](#), which permits use, distribution and reproduction for non-commercial purposes, provided the original is properly cited and derivative works building on this content are distributed under the same license.

IntechOpen

IntechOpen